

**JAERI-Research
2005-007**



JP0550107



**EVALUATION OF RF PROPERTIES BY ORIFICE
DESIGN FOR IFMIF RFQ**

March 2005

Sunao MAEBARA, Shin-ichi MORIYAMA,
Mikio SAIGUSA* and Masayoshi SUGIMOTO

日本原子力研究所
Japan Atomic Energy Research Institute

本レポートは、日本原子力研究所が不定期に公刊している研究報告書です。
入手の問合わせは、日本原子力研究所研究情報部研究情報課（〒319-1195 茨城県那珂郡東海村）あて、お申し越しください。なお、このほかに財団法人原子力弘済会資料センター（〒319-1195 茨城県那珂郡東海村日本原子力研究所内）で複写による実費頒布をおこなっております。

This report is issued irregularly.

Inquiries about availability of the reports should be addressed to Research Information Division, Department of Intellectual Resources, Japan Atomic Energy Research Institute, Tokai-mura, Naka-gun, Ibaraki-ken 319-1195, Japan.

© Japan Atomic Energy Research Institute, 2005

編集兼発行 日本原子力研究所
印刷 (株)高野高速印刷

Evaluation of RF Properties by Orifice Design for IFMIF RFQ

Sunao MAEBARA, Shin-ichi MORIYAMA⁺, Mikio SAIGUSA^{*} and Masayoshi SUGIMOTO

Department of Fusion Engineering Research

(Tokai Site)

Naka Fusion Research Establishment

Japan Atomic Energy Research Institute

Tokai-mura, Naka-gun, Ibaraki-ken

(Received January 27, 2005)

Orifices for the IFMIF RFQ have been designed and fabricated, and RF properties have been evaluated by a network analyzer. The designed orifices were installed into a vacuum port of the 1.1m-long RFQ mock-up module, and the resonant frequency and the phase difference between cavities were measured for a quadrupole operation mode of TE₂₁₀. It was found that the RF properties are not affected on condition that slit direction with the same direction of current flow at the RFQ wall. Orifice conductance from 0.22 to 0.25 m³/sec by nitrogen conversion at room temperature was designed, and an ultimate pressure level of 5x10⁻⁷ [Pa] was evaluated for the 4.1m-long central module for the IFMIF RFQ. It was concluded that the designed orifices are effective for RF properties and vacuum conductance in the IFMIF RFQ.

Keywords: IFMIF, RFQ, Orifice, RF Properties

⁺Department of Fusion Facility

^{*} Ibaraki University

IFMIF 用 RFQ のためのオリフィス・デザインに対する RF 特性評価

日本原子力研究所那珂研究所核融合工学部
前原 直・森山 伸一⁺・三枝 幹雄^{*}・杉本 昌義

(2005 年 1 月 27 日受理)

IFMIF(国際核融合材料中性子中性子照射施設)用 RFQ (高周波四重極加速器) のためのオリフィスを設計及び製作し、ネットワークアナライザーによる高周波特性の評価を行った。その設計されたオリフィスは、軸長さ 1.1m の RFQ モックアップモジュールに設置され、四重極運転モード TE₂₁₀ に対する共振周波数およびキャビティ間の位相差を測定した。この結果、オリフィスのスリット方向を RFQ 壁に流れる電流方向と同じにした条件では、高周波特性はオリフィスによる影響を受けないことが判明した。これらの設計されたコンダクタンスは、0.22 から 0.25 m³/sec であり、IFMIF RFQ における 4.1 m のセントラルモジュールにおいて、到達真空度は 5x10⁻⁷ [Pa]レベルとなることが見積もられた。設計したオリフィスが IFMIF 用 RFQ として RF 特性および真空コンダクタンスに対して有効である結論に達した。

Contents

1. Introduction	1
2. IFMIF RFQ	1
2.1 Conceptual Design of IFMIF RFQ	1
2.2 Design of RFQ Mock-up Module	3
2.3 Low Power Test of RFQ Mock-up Module	3
2.4 Higher Modes Analysis	4
3. RF Properties by Orifice Design	4
3.1 Orifice Design	4
3.2 RF Properties by Low Power Test	5
3.3 Evaluation of Ultimate Pressure	9
3.4 Future Investigation	9
4. Summary	10
Acknowledgement	10
Reference	10

目次

1. 序論	1
2. IFMIF RFQ	1
2.1 IFMIF RFQ の概念設計	1
2.2 RFQ モックアップモジュールの設計	3
2.3 RFQ モックアップモジュールの低電力試験	3
2.4 高次モードの解析	4
3. オリフィス設計に対する RF 特性	4
3.1 オリフィス設計	4
3.2 低電力試験による高周波特性	5
3.3 到達真空度の評価	9
3.4 次の課題	9
4. まとめ	10
謝辞	10
参考文献	10

This is a blank page.

1. Introduction

The International Fusion Materials Irradiation Facility (IFMIF) is an accelerator-based neutron irradiation facility to develop materials for a demonstration fusion reactor after ITER project[1-3]. For this purpose, materials have to be studied in radiation of more than 80 dpa, an intense neutron field equivalent to D-T fusion reactor environment using a deuteron-lithium (D-Li) stripping reaction.

In this system, a 40MeV deuteron beam with a current of 250mA is injected into liquid lithium flow with a speed of 20 m/s, and neutron field similar to D-T fusion reactor (2MW/m^2 , >20 dpa /year for Fe) is produced by the D-Li stripping reaction. The required current of 250mA is realized by two beam lines of 125mA, and the output energies at injector, radio-frequency quadrupole (RFQ) linac[4-5] and drift tube linac (DTL) are designed to be 0.1, 5.0 and 40.0 MeV, respectively[6]. CW operation is required for this system to obtain a high neutron fluence accumulation.

In such a CW RFQ linac, vacuum pressure of 10^{-7} [Pa] level seems to be needed to avoid beam scattering by residual gasses, but the effect has not been evaluated sufficiently for a large deuteron beam of 125mA. When an RFQ structure is made in a hole for vacuum port, the boundary condition for electromagnetic fields strictly changes. RF properties which are a resonant frequency and phase differences between quadrant cavities for the quadrupole operation mode (TE_{210}), are affected. In order to avoid these defects, an orifice design with an improved boundary condition, is indispensable. In this report, five kinds of orifice have been designed and fabricated. These orifices were installed into vacuum ports of an RFQ mock-up module, and RF properties have been evaluated by a low power test of Network Analyzer.

In section 2, a conceptual design of IFMIF RFQ, a design of the RFQ mock-up module, a low power test and higher modes analysis are outlined to assist for understanding. In section 3, orifice design, low power tests and the evaluation of pressure rise are presented. The last section provides conclusion.

2. IFMIF RFQ

2.1 Conceptual design of IFMIF RFQ

In the RFQ linac, the 12m-long RFQ was designed to accelerate the deuteron beam up to 5MeV. The operation frequency of 175MHz was selected to accelerate a large current of 125mA. The injection total RF power of 2.3 MW is needed. The configuration of the IFMIF

RFQ conceptual design is shown in Fig.2.1. In the 12m-long RFQ, suppression of higher modes are indispensable, and a coupled cavity technique will be used. The coupled cavity technique was developed for the 350 MHz RFQ system in APT/LEDA project of LANL[7-10], and central modules which have a short longitudinal length, are connected through the coupling plates as indicated in Fig.2.1.

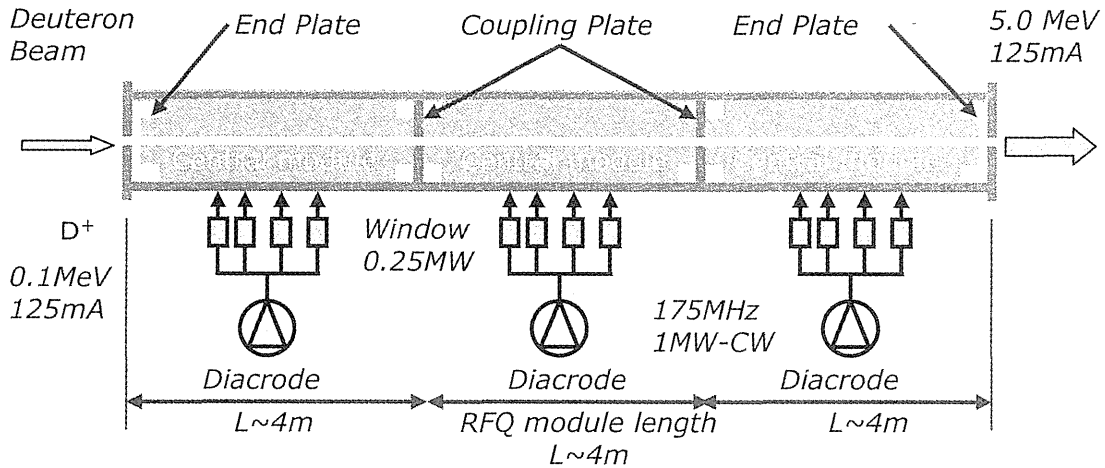


Fig.2.1 The configuration of IFMIF RFQ conceptual design

In the case that an RF input-coupler using conventional Iris type for the 175MHz frequency is designed, a rectangular waveguide of 1.0 x 0.5 m for a transmission line and a tapered rigid waveguide to decrease cut-off frequency in order to radiate RF power from small aperture, are needed as shown in Fig.2.2. Therefore, an RF-Input coupler using a loop antenna with co-axial transmission line has been developed.

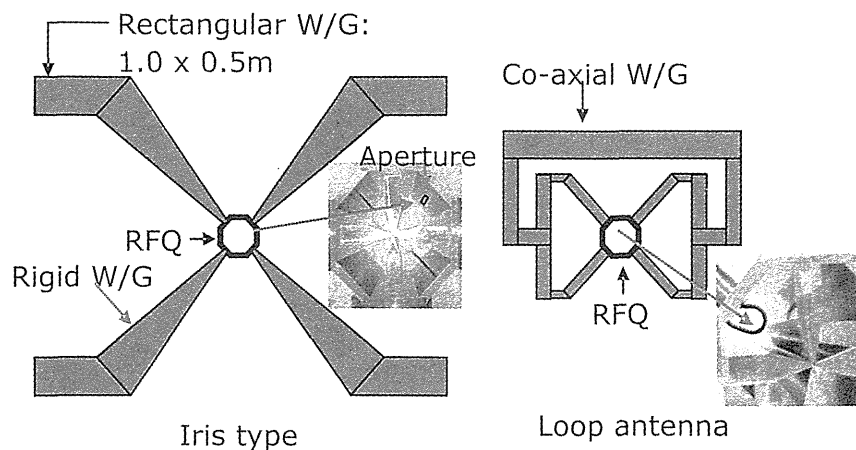


Fig.2.2 Transmission line system in case of using Iris type and Loop antenna for RF Input coupler

2.2 Design of RFQ mock-up module

The four-vane RFQ mock-up module had been designed by MAFIA[11] code before[12]. The RFQ module consists of two end-plate modules and central modules, and each end-plate module is connected to each side of central module. For this mock-up, the vanes have no modulation. The beam bore diameter and the vane radius were designed by a beam dynamics simulation code, and they were specified to be 8mm and 4mm, respectively. The resonant frequency was analyzed by changing each cavity dimension. After the cavity dimensions was finalized (as indicated in Fig.2.3), the central module and the two end-plate modules were fabricated with aluminum. Photographs of the central module and the end-plate module are shown in Fig.2.4. The gap between end-plate flange and the vane edge is 40mm, and the undercut area of the vane is 50mm from the edge in axial length and 82mm in radial direction from the vane root contacting the outer cavity frame. These dimensions were determined so that the electric field strength change at the vane edge from that at the center of central module, is suppressed to within 1%, and electric field uniformity around the tip of vane in the longitudinal direction is achieved.

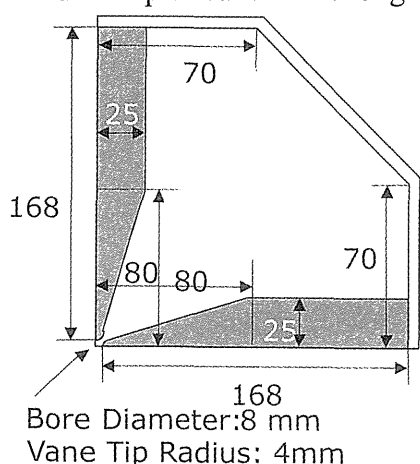


Fig.2.3 Dimension of the 175MHz RFQ mock-up cavity

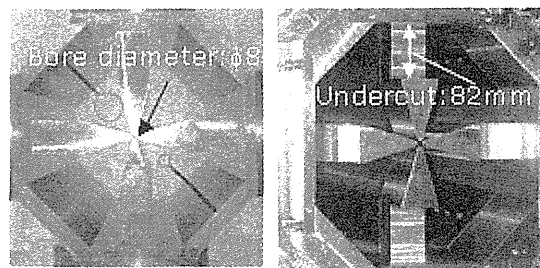


Fig.2.4 Photograph of central module (left) and end-plate module (right)

2.3 Low power test of RFQ mock-up module

The resonant frequency of the 1.1m-long RFQ module (Fig.2.5) was measured by a network analyzer. As shown in Fig.2.4 (left), a large loop antenna and a small pick-up coil which were made of $\phi 2$ mm wire, were used to reduce detuning of resonant frequency. The measured result is shown in Fig.2.6. The resonant frequency of 175.65 MHz for quadrupole operation mode (TE_{210}) was obtained, and it was in good agreement with the calculated value of 174.36MHz. This difference was less than 1% of the operation mode frequency. This difference is supposed to be caused by misalignment at the connection between central module and end-plate modules.

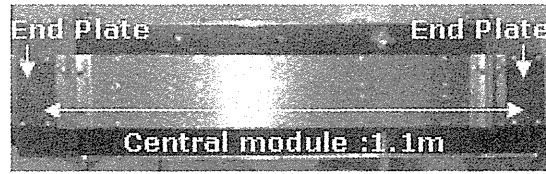


Fig.2.5 Photograph of the 1.1m-long RFQ module

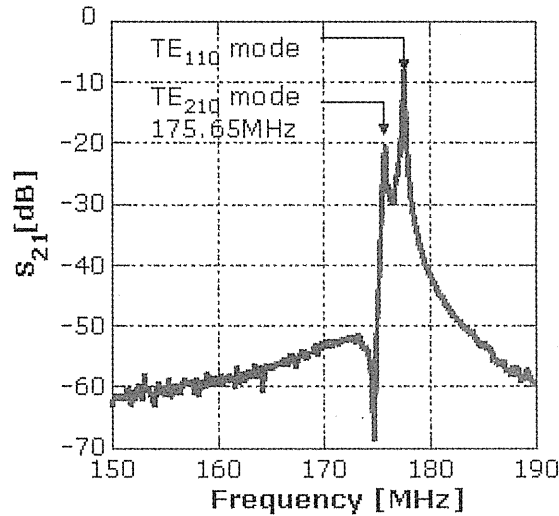


Fig.2.6 Measured resonant frequency of the 1.1m-long RFQ module

2.4 Higher modes analysis

Since measured resonant frequencies were in good agreement with the calculated values, higher modes as a function of a longitudinal length up to 4.1m were analyzed [12]. For the 4.1m-long RFQ, resonant frequencies of the TE_{210} and the TE_{111} modes were 173.91 MHz and 176.18 MHz, respectively. The difference was 2.27 MHz, it was assessed that the operation mode is not affected by the TE_{110} mode. It was also found that the difference of more than 1.54 MHz is obtained by the RFQ length of more than 2.1m, and operation mode is not affected. But the RFQ system design using 2, 3 and 5 coupling plates is considerable in this result, the RFQ design using two coupling plates will a good candidate from a low cost-effectiveness point of view.

3. RF properties by orifice design

3.1 Orifice design

Five kinds of orifice have been designed and fabricated. The orifice diameter was $\phi 60$ mm, and the aperture width of 4, 6 and 8 mm and slit width of 1 and 2 mm were designed as indicated in Fig.3.1 and Table 3.1. These orifices were installed into vacuum ports which make a hole in the RFQ quadrant wall as shown in Fig. 3.2. These conductance from 221 to 246 liter /sec by nitrogen conversion at room temperature were calculated.

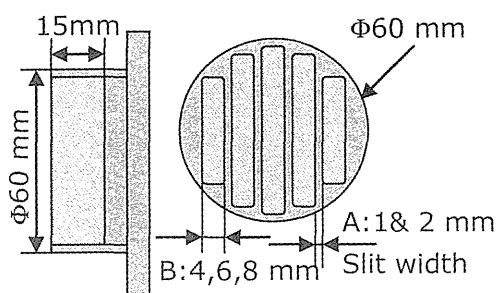


Fig.3.1 Vacuum port dimension

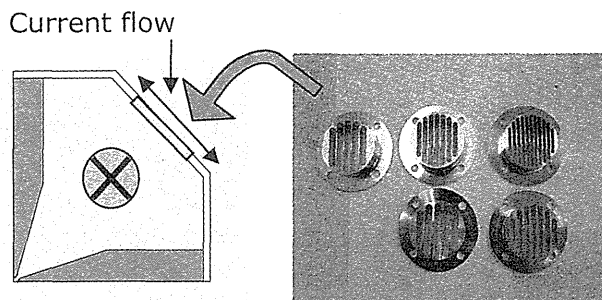


Fig.3.2 Installation of Vacuum port

Table 3.1 Dimension of orifice design

Case	A[mm]	B[mm]	Ratio[%]	C [liter/sec]
T1	1	4	65	221
T2	1	6	73	246
T3	1	8	71	238
T4	2	6	68	229
T5	2	8	68	229

A: Slit width, B: Aperture width, Ratio: Total area of aperture / Port area

C: Conductance by Nitrogen conversion at room temperature

3.2 RF properties by low power test

The experimental setup is shown in Fig.3.3. A large loop-antenna ($\phi 60\text{mm}$) and a small four pick-up coils ($\phi 10\text{mm}$) made of $\phi 2\text{mm}$ wire, were used to reduce detuning of a resonant frequency. The large loop antenna was used for an RF input coupler and installed at the center of the mock-up module. This antenna was connected to a co-axial waveguide end. RF signal from a network analyzer is injected into the RFQ mock-up module. Four pick-up coils were mounted for each cavity at the same position of 0.40m far from the module center. The S_{21} parameters (a transmission coefficient) for each cavity were measured, and the resonant mode was evaluated. Vacuum ports were made a hole at the position of 0.25m far from the module center. Not to cut current flow at RFQ quadrant wall for the operation mode (TE_{210}), the slit direction was set at the same direction of the current flow.

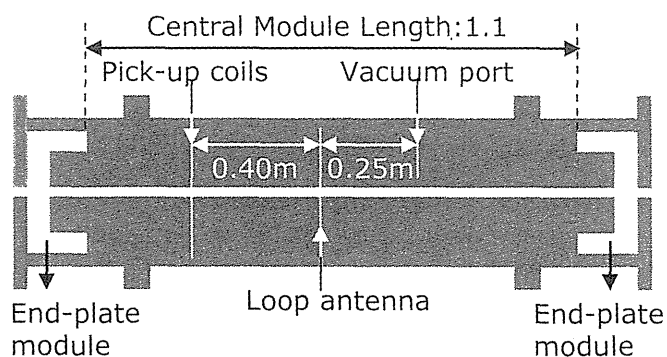


Fig.3.3 Experimental set-up for a low power test

When either one of each orifice (T1~T5) or a cover without slit aperture(No) was installed into the vacuum port, the reflection co-efficient (S_{11}) and the phase difference between Cavity #1 and #3 were measured. In Fig.3.4, it was found that the first peak in a low frequency at 177.8MHz is quadrupole operation mode (TE_{210}) by the phase differences between Cavity #1 and #3. Since the phase difference between Cavity #1 and #3 for the TE_{21n} modes is ideally 0° , and that for the dipole mode (TE_{10n}) is 180° . It was also found that the third peak in a high frequency at 179.1MHz is the dipole mode (TE_{110}), and the second peak is an overlap of modes. In all cases, the measured reflection co-efficient was almost the same, and it was found that RF properties are not affected by installing any one of orifices. As shown in Fig.3.5, no deviation was also found for the phase differences.

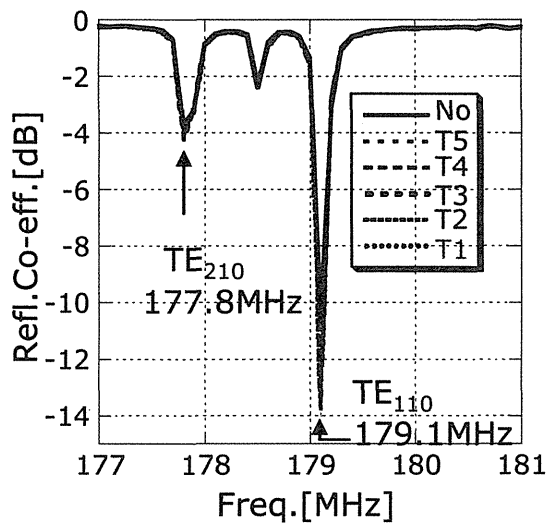


Fig.3.4 Reflection Co-efficient (S_{11}) of Large Loop antenna.

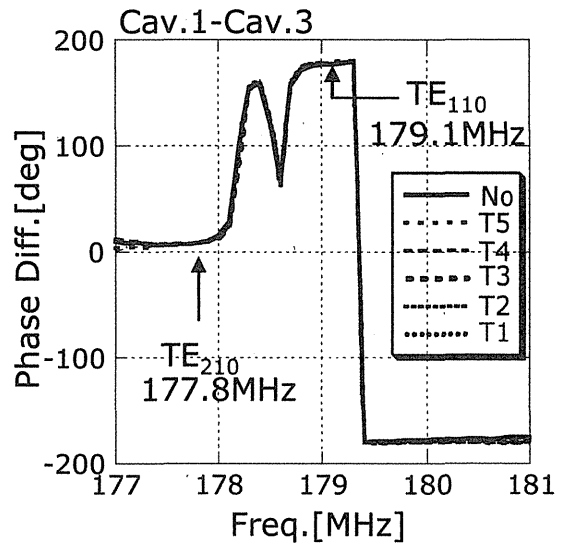


Fig.3.5 Phase difference between Cavity #1 and #3

In these measurements, the resonant frequency was increased in comparison with 175.65 MHz in Fig.2.4. This difference is supposed to be caused by distortion of the RFQ structure. Since both four vacuum ports with diameter of $\phi 60$ mm and RF input ports with diameter of $\phi 90$ mm were provided for each RFQ quadrant wall, these RFQ walls might be bent into inward direction. Then, the RFQ volume was decreased, and the resonant frequency was increased from 175.65MHz to 177.8MHz.

RF properties were also measured by changing angle of 90° with respect to the direction of current flow at the RFQ wall (T2-90 in Fig.3.6), or removing a port cover (WO in Fig.3.6).

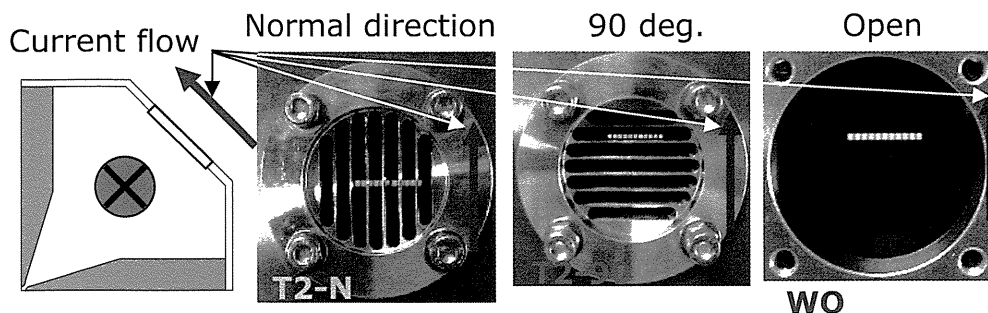


Fig.3.6 Current direction of RFQ wall and slit direction

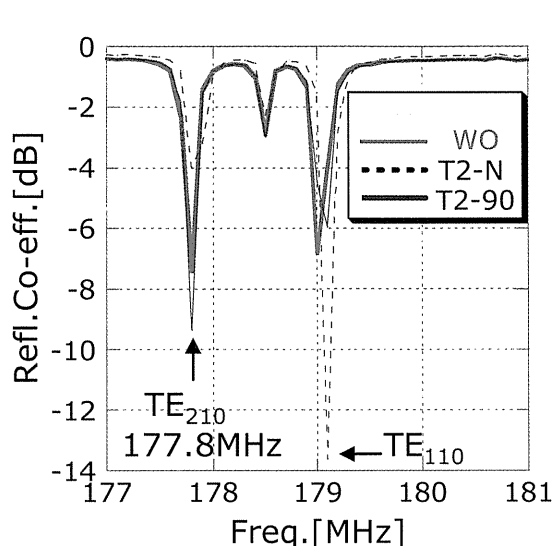
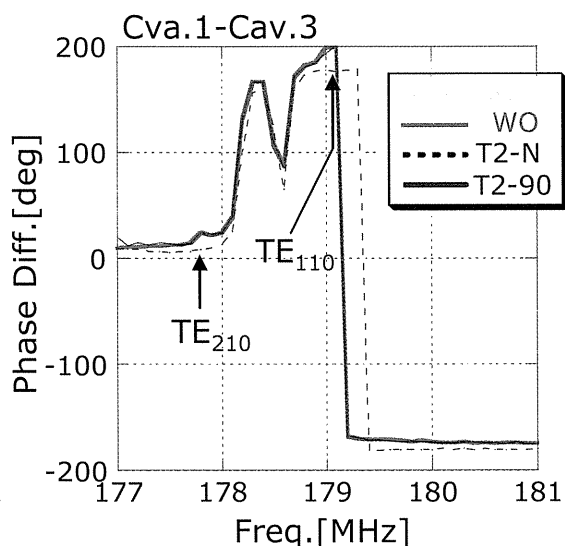
Fig.3.7 Reflection Co-efficient (S_{11}) of Large Loop antenna

Fig.3.8 Phase difference between Cavity #1 and #3

The measured results are shown in Fig.3.7 and Fig.3.8. The slit direction with the same direction of the current flow (T2-N), and a cover without slit aperture (No) are also presented. RF properties of T2-90 and WO were clearly changed in comparison with those of T2-N and No. In the T2-90, the reflection co-efficient of TE_{210} mode at 177.8 MHz was drastically changed from -4dB to -9.5dB by the slit direction, and the phase difference was also changed from 4° to 27° . Not to be affected by installing orifice, it was found that slit direction has to be set as the same direction as current flow direction at the RFQ wall for the TE_{210} mode.

When four orifices (T1~T4) were installed into all four vacuum ports, RF properties were also measured. These slits directions were set the same direction of the current flow. In Fig.3.9, the data using four orifices represents 4VP. In comparison with NO in the case that four vacuum ports are covered, the phase differences were almost same. It was found that RF properties are not affected at all by installing four orifices on condition that slit

This is a blank page.

directions are the same direction of the current flow at the RFQ wall for the TE₂₁₀ mode.

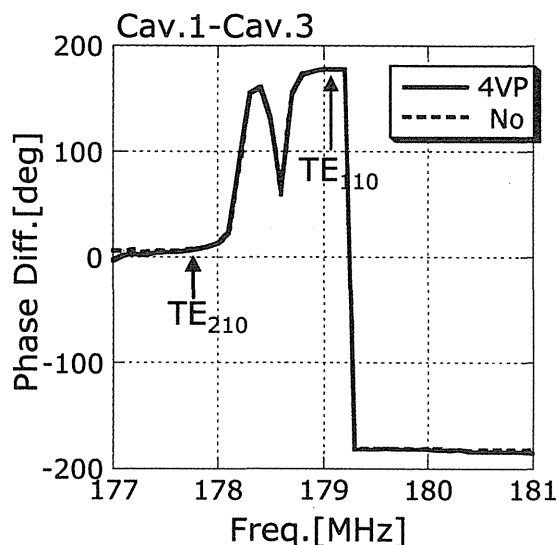


Fig.3.9 Phase difference between Cavity #1 and #3 when four orifices (T1~T4) are installed into all four vacuum ports

3.3 Evaluation of ultimate pressure

IFMIF RFQ will be made of copper material, because of suppression of RF losses. The outgassing rate (Q) from copper material already had been evaluated in several fields, and the rate (Q) of 5×10^{-8} [Pa m³/s m²] at the temperature of 50 C° was used. This rate is indicated after sufficient baking treatment and RF conditioning. The surface area for a quadrant RFQ of the 4.1m-long is about 2.4 m², and the outgassing flux(q) of 1.2×10^{-7} [Pa m³/s] is obtained. Using the obtained the flux(q), an ultimate pressure P_0 can be calculated by the equation of $P_0 = q/S$, where S and q represent pumping speed and the outgassing flux, respectively. When the pumping speed is assumed to be the same level as the orifice conductance of 0.23 [m³/s], an ultimate pressure (P_0) of 5.0×10^{-7} [Pa] is obtained. This ultimate pressure is low enough for the CW RFQ vacuum. It was found that these designed orifices are an effective for vacuum conductance.

3.4 Future investigation

There are three possibilities for the further steps. One is to establish water cooling method of the orifice in order to avoid the temperature rise. However, this cooling method already had been established at LANL for the 350 MHz CW RFQ system in APT/LEDA project, it seem to be easy to applied their technique. The second one is to evaluate an RF leak from orifice to vacuum pumping site. This is indispensable to avoid partial temperature rise in vacuum pumping system, and the RF leak evaluation at just front of vacuum pump at the RF injection power of 1kW level, is planned. The last one is suppression of gas flow from Light Energy Beam Transport system [LEBT] to RFQ system. Since the pressure level of 10^{-3} [Pa]

is used to cancel out beam space charge effect. In the case that the diameter 10mm for RFQ inlet aperture is made in a hole, the gas flow from LEBT of 9 [liter/sec] is expected. An additional pumping for this suppress seems to be needed at the end-plate part of RFQ.

4. Summary

Five kinds of orifice have been designed and fabricated. These orifices were installed into the vacuum ports of the 1.1m-long RFQ mock-up module, and RF properties which are a reflection co-efficient and phase differences between cavities for the quadrupole operation mode of TE_{210} , were measured by a network analyzer. When one of the orifices is installed into the vacuum on condition that the slit direction with the same direction of current flow for the TE_{210} mode, the RF properties in any cases were not altered from the results of a cover without slit aperture (No). However, the RF properties are affected by changing the slit direction of 90° . Moreover, four orifices were installed into the vacuum ports, the all slit direction was set the same direction of current flow. It was also found that RF properties are not affected at all. In the 4.1m-long RFQ central module, an ultimate pressure (P_0) of 5.0×10^{-7} [Pa] was evaluated. This ultimate pressure is low enough for the CW RFQ vacuum. It was concluded that these designed orifices are effective for RF properties and for vacuum conductance in the IFMIF RFQ.

Acknowledgement

The authors wish to express their thanks to Drs. T.Imai, H. Takatsu and S. Seki for their discussion and their useful comments. The authors also thank their colleagues from the Plasma Heating Laboratory and the RF Facility Division in JAERI for their continuous support.

Reference

- [1] IFMIF-CDA Team (Ed.) M. Martone, "IFMIF Conceptual Design Activity Final Report", *ENEA Frascati Report*, RT/ERG/FUS/96/17 (1996).
- [2] T. Kondo et al., "IFMIF, its facility concept and technology", *J.of Nuc. Mater.*, 258-263,47(1998).
- [3] T. E. Shannon et.al., "Conceptual design of the international fusion materials irradiation facility(IFMIF)", *J. of Nucl. Mater.*, 106(1998).
- [4] M. Kapchinskiy and V. A. Teplyaikov, "Linear accelerator with spatially homogeneous strong focusing", *Prib. Tekh. Eksp.* 2, 19-22(1970).
- [5] K. R. Crandall et al., "RF Quadrupole beam dynamic design studies", *Proc. the 1979 Linear Accelerator Conf.*, Mantauk, New York, Sep 10-14, vol.3, p.205(1979).
- [6] IFMIF Internal Team, "IFMIF-KEP Report", *JAERI, JAERI-Tech 2003-005*, March 2003
- [7] D. Schrage, et al., "CW RFQ Fabrication and Engineering", *Proc. the XIX Int. LINAC*

- Conf.*, Chicago, Aug 23-28, p.679-683(1998).
- [8] L. M. Young, et al., "High-Power Operation of LEDA", *Proc. the XX Int. LINAC Conf.*, Monterey, Aug 21-25, p.336-340(2000).
- [9] L. M. Young et al., "Operations of the LEDA Resonantly Coupled RFQ", *Proc. of the 2001 Particle Accelerator Conf.*, Chicago, Illinois U.S.A., June 18-22, p.309-313(2001).
- [10] H. V. Smith, Jr. et al., "Low-Energy Demonstration Accelerator (LEDA) Test Results and Plans", *Proc. the 2003 Particle Accelerator Conf.*, Chicago, Illinois U.S.A., June 18-22, p.3296-3298(2001).
- [11] MAFIA4, CST, GmbH, Darmstadt, Germany
- [12] S. Maebara et al., "Low power test of RFQ mock-up modules at 175MHz for IFMIF RFQ", *Proc. of the 2003 Particle Accelerator Conf.*, Portland, Oregon U.S.A., May 12-16, p2829-2831(2003).

This is a blank page.

国際単位系 (SI) と換算表

表 1 SI 基本単位および補助単位

量	名 称	記 号
長 さ	メ ー ト ル	m
質 量	キ ロ グ ラ ム	kg
時 間	秒	s
電 流	ア ン ペ ア	A
熱力学温度	ケ ル ビ ン	K
物 質 量	モ ル	mol
光 度	カ ン デ ラ	cd
平 面 角	ラ ジ ア ン	rad
立 体 角	ステラジアン	sr

表 3 固有の名称をもつ SI 組立単位

量	名 称	記号	他の SI 単位 による表現
周 波 数	ヘ ル ツ	Hz	s ⁻¹
力	ニ ュ ー ト ン	N	m·kg/s ²
圧 力, 応 力	パ ス カ ル	Pa	N/m ²
エネルギー, 仕事, 熱量	ジ ュ ー ル	J	N·m
工 率, 放 射 束	ワ ッ ト	W	J/s
電 気 量, 電 荷	ク ー ロ ン	C	A·s
電位, 電圧, 起電力	ボ ル ト	V	W/A
静 電 容 量	フ ァ ラ ド	F	C/V
電 気 抵 抗	オ ー ム	Ω	V/A
コンダクタンス	ジーメンズ	S	A/V
磁 束	ウ ェ ー バ	Wb	V·s
磁 束 密 度	テ ス ラ	T	Wb/m ²
インダクタンス	ヘ ン リ ー	H	Wb/A
セルシウス温度	セルシウス度	°C	
光 束	ル ー メ ン	lm	cd·sr
照 度	ル ク ス	lx	lm/m ²
放 射 能	ベ ク レ ル	Bq	s ⁻¹
吸 収 線 量	グ レ イ	Gy	J/kg
線 量 当 量	シーベルト	Sv	J/kg

表 2 SI と併用される単位

名 称	記 号
分, 時, 日	min, h, d
度, 分, 秒	°, ', "
リ ッ ト ル	l, L
ト ン	t
電子ボルト	eV
原子質量単位	u

$$1 \text{ eV} = 1.60218 \times 10^{-19} \text{ J}$$

$$1 \text{ u} = 1.66054 \times 10^{-27} \text{ kg}$$

表 4 SI と共に暫定的に
維持される単位

名 称	記 号
オンゲストローム	Å
バ ー ン	b
バ ー ル	bar
ガ ル	Gal
キ ュ リ ー	Ci
レ ン ト ゲ ン	R
ラ ド	rad
レ ム	rem

$$1 \text{ Å} = 0.1 \text{ nm} = 10^{-10} \text{ m}$$

$$1 \text{ b} = 100 \text{ fm}^2 = 10^{-28} \text{ m}^2$$

$$1 \text{ bar} = 0.1 \text{ MPa} = 10^5 \text{ Pa}$$

$$1 \text{ Gal} = 1 \text{ cm/s}^2 = 10^{-2} \text{ m/s}^2$$

$$1 \text{ Ci} = 3.7 \times 10^{10} \text{ Bq}$$

$$1 \text{ R} = 2.58 \times 10^{-4} \text{ C/kg}$$

$$1 \text{ rad} = 1 \text{ cGy} = 10^{-2} \text{ Gy}$$

$$1 \text{ rem} = 1 \text{ cSv} = 10^{-2} \text{ Sv}$$

表 5 SI 接頭語

倍数	接頭語	記 号
10 ¹⁸	エクサ	E
10 ¹⁵	ペタ	P
10 ¹²	テラ	T
10 ⁹	ギガ	G
10 ⁶	メガ	M
10 ³	キロ	k
10 ²	ヘクト	h
10 ¹	デカ	da
10 ⁻¹	デシ	d
10 ⁻²	センチ	c
10 ⁻³	ミリ	m
10 ⁻⁶	マイクロ	μ
10 ⁻⁹	ナノ	n
10 ⁻¹²	ピコ	p
10 ⁻¹⁵	フェムト	f
10 ⁻¹⁸	アト	a

(注)

- 表 1-5 は「国際単位系」第 5 版, 国際度量衡局 1985 年刊行による。ただし, 1 eV および 1 u の値は CODATA の 1986 年推奨値によった。
- 表 4 には海里, ノット, アール, ヘクタールも含まれているが日常の単位なのでここでは省略した。
- bar は, JIS では流体の圧力を表わす場合に限り表 2 のカテゴリーに分類されている。
- EC 閣僚理事会指令では bar, barn および「血圧の単位」mmHg を表 2 のカテゴリーに入れている。

換 算 表

力	N (=10 ⁵ dyn)	kgf	lbf
	1	0.101972	0.224809
	9.80665	1	2.20462
	4.44822	0.453592	1

$$\text{粘 度 } 1 \text{ Pa} \cdot \text{s} (\text{N} \cdot \text{s/m}^2) = 10 \text{ P (ポアズ)} (\text{g}/(\text{cm} \cdot \text{s}))$$

$$\text{動粘度 } 1 \text{ m}^2/\text{s} = 10^4 \text{ St (ストークス)} (\text{cm}^2/\text{s})$$

圧	MPa (=10 bar)	kgf/cm ²	atm	mmHg (Torr)	lbf/in ² (psi)
	1	10.1972	9.86923	7.50062 × 10 ³	145.038
力	0.0980665	1	0.967841	735.559	14.2233
	0.101325	1.03323	1	760	14.6959
	1.33322 × 10 ⁻⁴	1.35951 × 10 ⁻³	1.31579 × 10 ⁻³	1	1.93368 × 10 ⁻²
	6.89476 × 10 ⁻³	7.03070 × 10 ⁻²	6.80460 × 10 ⁻²	51.7149	1

エネルギー・仕事・熱量	J (=10 ⁷ erg)	kgf·m	kW·h	cal (計量法)	Btu	ft·lbf	eV
	1	0.101972	2.77778 × 10 ⁻⁷	0.238889	9.47813 × 10 ⁻⁴	0.737562	6.24150 × 10 ¹⁸
	9.80665	1	2.72407 × 10 ⁻⁶	2.34270	9.29487 × 10 ⁻³	7.23301	6.12082 × 10 ¹⁹
	3.6 × 10 ⁶	3.67098 × 10 ⁵	1	8.59999 × 10 ⁵	3412.13	2.65522 × 10 ⁶	2.24694 × 10 ²⁵
	4.18605	0.426858	1.16279 × 10 ⁻⁶	1	3.96759 × 10 ⁻³	3.08747	2.61272 × 10 ¹⁹
	1055.06	107.586	2.93072 × 10 ⁻⁴	252.042	1	778.172	6.58515 × 10 ²¹
	1.35582	0.138255	3.76616 × 10 ⁻⁷	0.323890	1.28506 × 10 ⁻³	1	8.46233 × 10 ¹⁸
	1.60218 × 10 ⁻¹⁹	1.63377 × 10 ⁻²⁰	4.45050 × 10 ⁻²⁶	3.82743 × 10 ⁻²⁰	1.51857 × 10 ⁻²²	1.18171 × 10 ⁻¹⁹	1

$$1 \text{ cal} = 4.18605 \text{ J (計量法)}$$

$$= 4.184 \text{ J (熱化学)}$$

$$= 4.1855 \text{ J (15 °C)}$$

$$= 4.1868 \text{ J (国際蒸気表)}$$

$$\text{仕事率 } 1 \text{ PS (仏馬力)}$$

$$= 75 \text{ kgf} \cdot \text{m/s}$$

$$= 735.499 \text{ W}$$

放射能	Bq	Ci
	1	2.70270 × 10 ⁻¹¹
	3.7 × 10 ¹⁰	1

吸収線量	Gy	rad
	1	100
	0.01	1

照射線量	C/kg	R
	1	3876
	2.58 × 10 ⁻⁴	1

線量当量	Sv	rem
	1	100
	0.01	1

(86 年 12 月 26 日現在)

